Reaction of Ketenyl Radical with Acetylene: A Promising Route for Cyclopropenyl Radical

Hong-bin Xie, Yi-hong Ding,* and Chia-chung Sun

State Key Laboratory of Theoretical and Computational Chemistry, Institute of Theoretical Chemistry, Jilin University, Changchun 130023, People's Republic of China

Received: February 16, 2006; In Final Form: April 5, 2006

The reaction of the ketenyl radical (HCCO) with acetylene (C_2H_2) is very relevant to the oxygen−acetylene flames and fuel-rich combustion process for nitrogen-containing compounds. Unfortunately, except for several rate constant measurements, the mechanism is completely unknown for this reaction. In this paper, detailed theoretical investigations are performed for the HCCO + C_2H_2 reaction at the G3B3 level using the B3LYP/6-31G(d), B3LYP/6-311++G(d,p), and QCISD/6-31G(d) geometries. The exclusive fragmentation channel is the formation of the cyclopropenyl radical (*c*-C_3H_3) and carbon monoxide (CO) via the chainlike OCCHCHCH and three-membered ring OC−cCHCHCH intermediates. Thus, the mass spectroscopic peak of $C_3H_3^+$ in a previous experiment can be explained. The calculated overall reaction barrier is 4.4, 4.4, and 5.3 kcal/mol at the G3B3//B3LYP/6-31G(d), G3B3//B3LYP/6-311++G(d,p), and G3B3//QCISD/6-31G(d) levels, respectively. The title reaction may provide an effective route for generating the long-sought cyclopropenyl radical in the laboratory, which has been the long-standing subject of numerous theoretical studies as the simplest cyclic conjugate radical, and its bulky derivatives were already known. Future experimental investigations for the HCCO + C_2H_2 reaction are greatly desired to test the predicted fragmentation channel. The implication of the present study in combustion and interstellar processes is discussed.

1. Introduction

Several important phenomena of hydrocarbon combustion (ultraviolet[1] and visible[2,3] chemiluminescence, soot,[4−6] chemiions,[7,8] and both prompt formation[9] and removal[10−13] of nitric oxide) have a complex series of reactions at their root driven by small and highly reactive hydrocarbon radicals.[14] Of these reactions, those involving the ketenyl radical, HCCO, play a central role.[14] On the other hand, HCCO has been predicted to be of importance in astrophysical chemistry.[15] Besides helium, H, C, and O are known to be the former-three abundant elements in space. Up to now, more than 14 species composed of H, C, and O have been detected in space, that is, HCO, H_2CCO, HCCCHO, and so forth.[16] Although the HCCO radical itself still remains unknown in space, its potential existence has been postulated.[15] Detection of HCCO is just a matter of time. Therefore, the formation and depletion mechanisms of the HCCO radical are of great interest. Up to now, a large number of experimental and theoretical studies have been reported on the spectroscopic properties[17−23] of HCCO and its reactions.[24−29]

Among the HCCO reactions, the reaction with acetylene (C_2H_2) attracts our great interest. In the oxidation of C_2H_2 by O atoms, it has been acknowledged that HCCO (plus H) is the main product despite some quantitative disputes in the branching ratio with CH_2 + CO.[28] In the NCO reactions with alkynes such as C_2H_2, HCCO is also the predominant product.[30,31] Surely, the removal mechanism of the HCCO radical toward the abundant C_2H_2 is important to understand the whole evolution processes of the O/C_2H_2 and NCO/alkynes systems as well as the decay rates of the HCCO radicals. The title reaction may be particularly important in the high abundance of C_2H_2. Several experimental studies have reported the upper bound rate constants of the HCCO + C_2H_2 reaction.[25] To our surprise, the mechanism is completely unknown. Only in one early experimental study on the oxidation of acetylene by atomic oxygen was there an indication of the C_3H_3 formation on the basis of the mass spectroscopic peak of $C_3H_3^+$. It was proposed that C_3H_3 may originate both from the $^3CH_2$ + C_2H_2 and HCCO + C_2H_2 reactions.[25] The C_3H_3 (in linear form) formation from the former reaction can find support from theoretical studies.[32] However, whether the HCCO + C_2H_2 reaction can actually lead to the C_3H_3 radical, whether C_3H_3 possesses the linear or cyclic structure, and to what degree the two reactions can contribute to the C_3H_3 formation are still uncertain. To the best of our knowledge, there have been no published theoretical studies on this reaction. It has now been accepted that the oxidation process of C_2H_2 is very complex due to the intervening between the generated radicals and the reactants. We feel that without the reliable mechanistic information of the HCCO + C_2H_2 reaction, it is very difficult to fully understand the C_2H_2 burning processes with either oxygen or NCO radicals.

In this paper, a detailed Gaussian-3 study based on the density functional theory and configuration interaction geometries is reported on the HCCO + C_2H_2 reaction. Interestingly, the most probable fragmentation channel is the formation of the cyclopropenyl radical (plus carbon monoxide), which is experimentally still unknown up to now. Yet, we argue that the cyclopropenyl radical may have been previously detected in one early experiment. The present study suggests that the HCCO + C_2H_2 reaction could provide an effective route for the long-sought cyclopropenyl radical.

2. Theoretical Methods

All calculations are carried out using the GAUSSIAN98 program package.[33] The optimized geometries and harmonic frequencies of the reactant, products, isomers, and transition states are initially calculated at the B3LYP/6-31G(d) level.

* Corresponding author. E-mail: yhdd@mail.jlu.edu.cn.

10.1021/jp061013n CCC: $33.50
Published on Web 05/11/2006

Connections of the transition states between designated local minima have been confirmed by intrinsic reaction coordinate (IRC) calculations at the B3LYP/6-31G(d) level. Single-point calculations of the reaction HCCO + C_2H_2 are performed using the composite G3B3 scheme.[34,35] For the typical G3B3 method, the B3LYP/6-31G(d)-optimized geometries and scaled B3LYP/6-31G(d) zero-point vibrational energies (ZPE) are used. The MP4(FC))/6-31G(d), MP4(FC)/6-31+G(d), MP4(FC)/6-31G-(2df,p), QCISD(T,FC)/6-31G(d), and MP4(FU)/G3MP2large single-point energy calculations are carried out. The spin-orbital (SO) correction and high-level correction (HLC) are also included. Thus, the total G3B3 energy can be expressed as

$$E(\mathrm{G3B3}) = E[\mathrm{MP4(FC)/6\text{-}31(d)}] + \Delta(+) + \Delta(\mathrm{2df,p}) + \Delta(\mathrm{QCI}) + \Delta + \Delta\mathrm{SO} + \Delta\mathrm{HLC} + \mathrm{ZPE}$$

where

$$\Delta(+) = E[\mathrm{MP4(FC)/6\text{-}31{+}G(d)} - \mathrm{MP4(FC)/6\text{-}31G(d)}]$$

$$\Delta(\mathrm{2d\ f,p}) = E[\mathrm{MP4(FC)/6\text{-}31G(2df,p)} - \mathrm{MP4(FC)/6\text{-}31G(d)}]$$

$$\Delta(\mathrm{QCI}) = E[\mathrm{QCISD(T,FC)/6\text{-}31G(d)} - \mathrm{MP4(FC)/6\text{-}31G(d)}]$$

$$\Delta = [\mathrm{MP2(FU)/G3large} - \mathrm{MP2(FC)6\text{-}31G(2df,p)} - \mathrm{MP2(FC)/6\text{-}31{+}G(d)} + \mathrm{MP2/6\text{-}31G(d)}]$$

The HLC is $-An_\beta - B(n_\alpha - n_\beta)$ for molecules, where n_α and n_β are the number of α and β valence electrons, respectively, with $n_\alpha \geq n_\beta$. The coefficients A and B are 6.760 and 3.233 mhartrees. The G3B3 average absolute deviation from experiment for the 299 energies is 0.99 kcal/mol, compared to 1.01 kcal/mol for G3 theory.

The B3LYP/6-311++G(d,p) calculations on geometries and frequencies are further performed for all species obtained at the B3LYP/6-31G(d) level. Using the B3LYP/6-311++G(d,p) structures and frequencies, the G3B3 scheme is also applied, denoted as G3B3//B3LYP/6-311++G(d,p). For comparison, the typical G3B3 method based on the B3LYP/6-31G(d) structures and frequencies is denoted as G3B3//B3LYP/6-31G(d).

Our choice of the B3LYP density functional is preliminarily motivated by its good performance for the geometry optimizations and prediction of vibrational frequencies for both minimum isomers and transition states based on our own experiences and many literatures.[36] Another important reason is that B3LYP can implicitly include electron correlation[37] and is usually subject to small spin contamination. The combination of B3LYP with a series of high-level single-point energy calculations as implemented in the G3B3 method has been proved to provide very accurate thermochemical energetics.[34,35]

We are also aware that the B3LYP level of theory has been demonstrated to be not so reliable when calculating transition states in some cases.[38] Thus, for the relevant species of the HCCO + C_2H_2 reaction, the cost-expensive QCISD/6-31G(d) geometrical calculations are carried out followed by the G3B3 energy calculations (denoted as G3B3//QCISD/6-31G(d)). Luckily, the B3LYP-based calculations are found to be reliable for this study.

3. Results and Discussions

Figure 1 depicts the structures of reactants, most important products, isomers, and transition states. The schematic potential energy surface (PES) of the HCCO + C_2H_2 reaction at the G3B3//B3LYP/6-31G(d) level is presented in Figure 2.

The total energy of the reactant **R** HCCO + C_2H_2 is set as zero. The energetic data for G3B3//B3LYP/6-31G(d) and G3B3//B3LYP/6-311++G(d,p) levels of products, isomers, and transition states for the HCCO + C_2H_2 reaction are listed in Table 1. The symbol **TSm/n** is used to denote the transition state connecting the isomers **m** and **n**. The symbols "**L**" and "**r**" are added to the Arabic number **m** to denote the chainlike and ring isomers, respectively. Unless otherwise notified, the G3B3//B3LYP/6-31G(d) energies are used throughout.

3.1. Entrance Channels. The attack of the HCCO radical on the C_2H_2 molecule may have three kinds of entrance pathways: (i) direct H-transfer to form H_2CCO + C_2H **P_7** (26.3), HOCCH + C_2H **P_{11}** (60.0), or C_2H_3 + ^{3}CCO **P_{10}** (64.3); (ii) O-addition to form **L5** HCCOCHCH (15.8) via **TSR/L5** (30.2), and (iii) α-C (neighboring to H)-addition to form HCCHCHCO **L1a** (−26.3) via **TSR/L1a** (4.4). The values in parentheses are G3B3//B3LYP/6-31G(d) relative energies in kcal/mol with reference to **R** (0.0). Surely, only the α-C-addition pathway (iii) is of interest in combustion. It is both thermodynamically and kinetically much more competitive than the other pathways. Note that the low-lying OCCHCHCH **L1** has four isomeric forms **L1a** (−26.3), **L1b** (−28.8), **L1c** (27.9), and **L1d** (27.4), which can easily be interconverted to each other with the barriers around or less than 4 kcal/mol. Optimization of the transition states **TSR/L1b**, **TSR/L1c**, and **TSR/L1d** cannot succeed and often leads to **TSR/L1a**.

The most favorable α-C-addition attack can find support from spin distribution and orbital analysis. The respective spin density of the HCCO radical is −0.0531, 0.891, −0.218, and 0.380e on H, α-C, β-C, and O. The α-C-atom with the most spin density should be the most reactive site. As shown in Figure 3, the LUMO orbital of HCCO is C−O π-antibonding and C−C π-bonding with greater density on the α-C-atom. The HOMO orbital of C_2H_2 is C−C π-bonding. At the B3LYP/6-31G(d) level, the frontier orbital energies are −0.27030, −0.15992, −0.28193, and 0.05243 au for $E(\mathrm{HOMO_{HCCO}})$, $E(\mathrm{LUMO_{HCCO}})$, $E(\mathrm{HOMO_{C_2H_2}})$, and $E(\mathrm{LUMO_{C_2H_2}})$, respectively. The absolute energy difference 0.12201 au between $E(\mathrm{LUMO_{HCCO}})$ and $E(\mathrm{HOMO_{C_2H_2}})$ is smaller than 0.32273 au between $E(\mathrm{HOMO_{HCCO}})$ and $E(\mathrm{LUMO_{C_2H_2}})$. Thus, according to frontier orbital theory, the interaction should take place between HCCO's LUMO and C_2H_2's HOMO. We note that for HCCO, the LUMO is the counterpart of SOMO and can accept only one electron from C_2H_2. Thus, formation of one bond between HCCO and C_2H_2 at a time is preferable, although [1 + 2] and [2 + 2] cycloaddition processes are both seemingly symmetry allowed. The [3 + 2] cycloaddition is already symmetry forbidden. In fact, the concerted transition states for the direct [2 + 2] and [3 + 2] cycloaddition to form the respective four- and five-membered ring isomers O−cCCHCHCH **r4** (−45.5) and cOC-CHCHCH **r5** (−33.2), respectively, cannot be located despite numerous attempts at various levels including B3LYP/6-31G(d), MP2/6-31G(d), and QCISD/6-31G(d). Surprisingly, a concerted [1 + 2] cycloaddition transition state in C_s symmetry to form OC−cCHCHCH **r3** (−17.4) is located at the MP2 level with various basis sets 6-31G(d), 6-31+G(d,p), and 6-311++G(d,p). This transition state lies 11.2 kcal/mol above the reactant at the MP2/6-311++G(d,p) level, showing the minute interest of this process. However, such a C_s-transition structure is only a second-order transition state (with two imaginary frequencies) at other levels including B3LYP/6-31G(d), B3LYP/6-311++G-(d,p), B3PW91/6-31G(d), BH&LYP/6-31G(d), MP3/6-31G(d), MP4SDQ/6-31G(d), and QCISD/6-31G(d). Relaxation of its symmetry leads to **TSL1d/r3**. Because the MP3, MP4SDQ, and QCISD methods contain higher electron correlation procedures than MP2, we conclude that such a transition state may actually

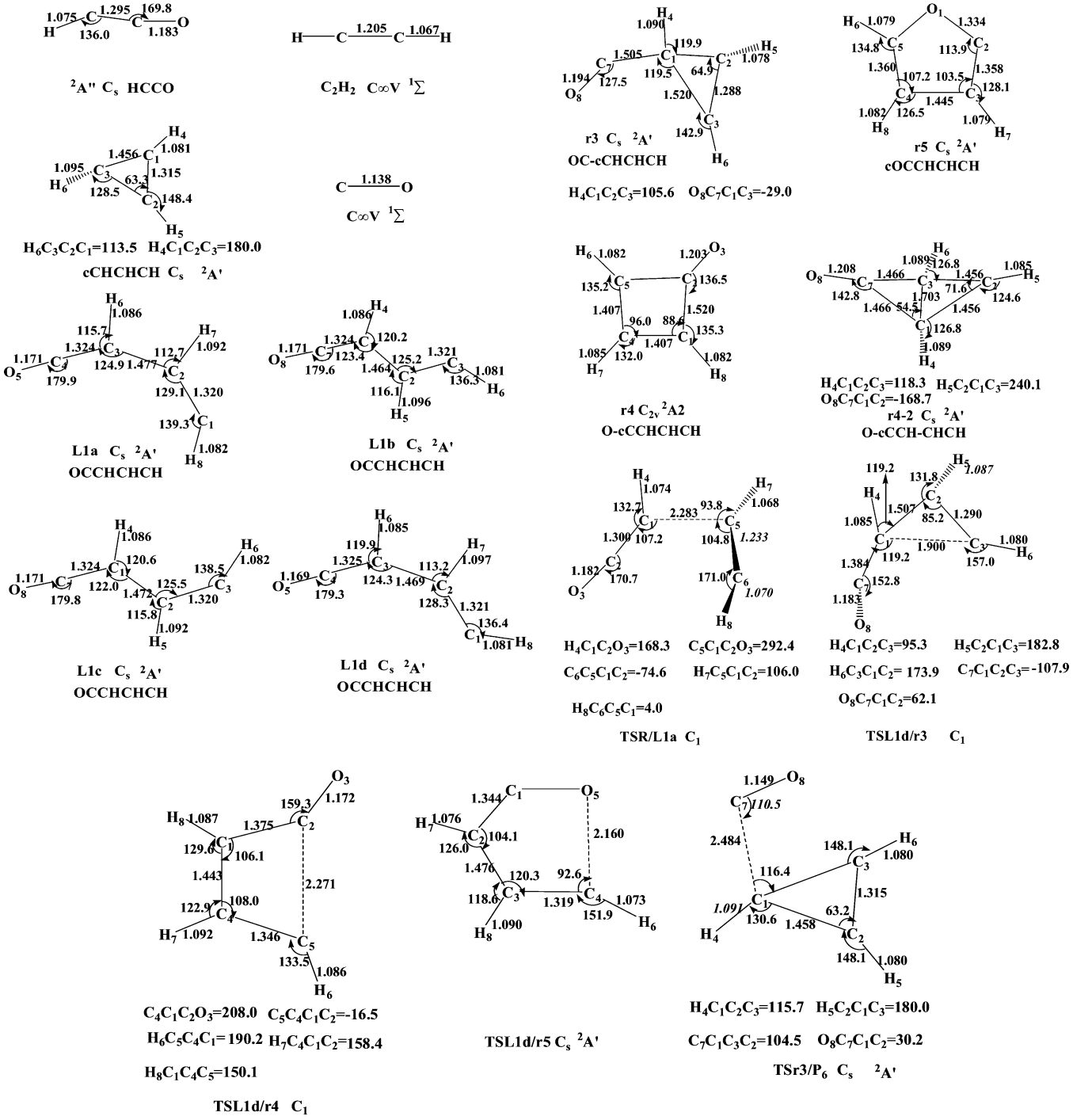

Figure 1. Optimized geometries of reactants, most important isomers, and interconversion transition states for the HCCO + C_2H_2 reaction at the B3LYP/6-31G(d), level. Bond lengths are in angstroms and angles in degrees.

not exist. It could be an artifact of the MP2 method. We also note that no concerted transition states for the direct [1 + 2], [2 + 2], and [3 + 2] cycloaddition to form the three-, four- and five-membered ring isomers have been located for both reactions HCCO + O_2[39] and NCO + C_2H_2.[40]

3.2. Isomerization and Dissociation. Starting from the most favorable entrance isomer HCCHCHCO **L1**, three kinds of pathways are identified: (i) ring-closure to form the three, four, and five-membered ring isomers OC−cCHCHCH **r3** (−17.4), O−cCCHCHCH **r4** (−45.5), and cOCCHCHCH **r5** (−33.2), respectively; (ii) H-shift to form the chainlike isomers OCCH-CCH_2 **L3** (−35.0) and $OCCH_2CCH$ **L7** (−33.8), (1,2-H-shift), $OCCCHCH_2$ **L4** (−38.8) and OCHCHCCH **L2** (−41.5) (1,3-H-shift), HCCCHCOH **L6** (−8.8) (1,4-H-shift); and (iii) H-extrusion to form $\mathbf{P_1}$ HCCCHCO + H (4.5). As shown in Figure 2, only the first kind of pathway forming ring isomers has the transition states, that is, **TSL1d/4r** (−12.3), **TSL1d/5r** (−1.6), and **TSL1d/3r** (−1.2), lower in energy than the entrance α-C-addition **TSR/L1a** (4.4) and the reactant **R**. Pathway (iii) is much less competitive with $\mathbf{TSL1d/P_1}$ (9.0) lying by 4.6 kcal/mol higher than **TSR/L1a** (4.4). The remaining pathways are even of neglectable competition due to the high-energy transition states **TSL1b/L2** (14.5), **TSL1b/L4** (15.2), **TSL1a/L3** (15.3), **TSL1b/L7** (25.2), and **TSL1b/L6** (26.8).

Starting from the low-lying intermediates **r4** O−cCCHCHCH (−45.5) and **r5** cOCCHCHCH (−33.2), there are several transform pathways, which can be generally divided into two kinds: direct H-extrusion and H-migration along the ring. For

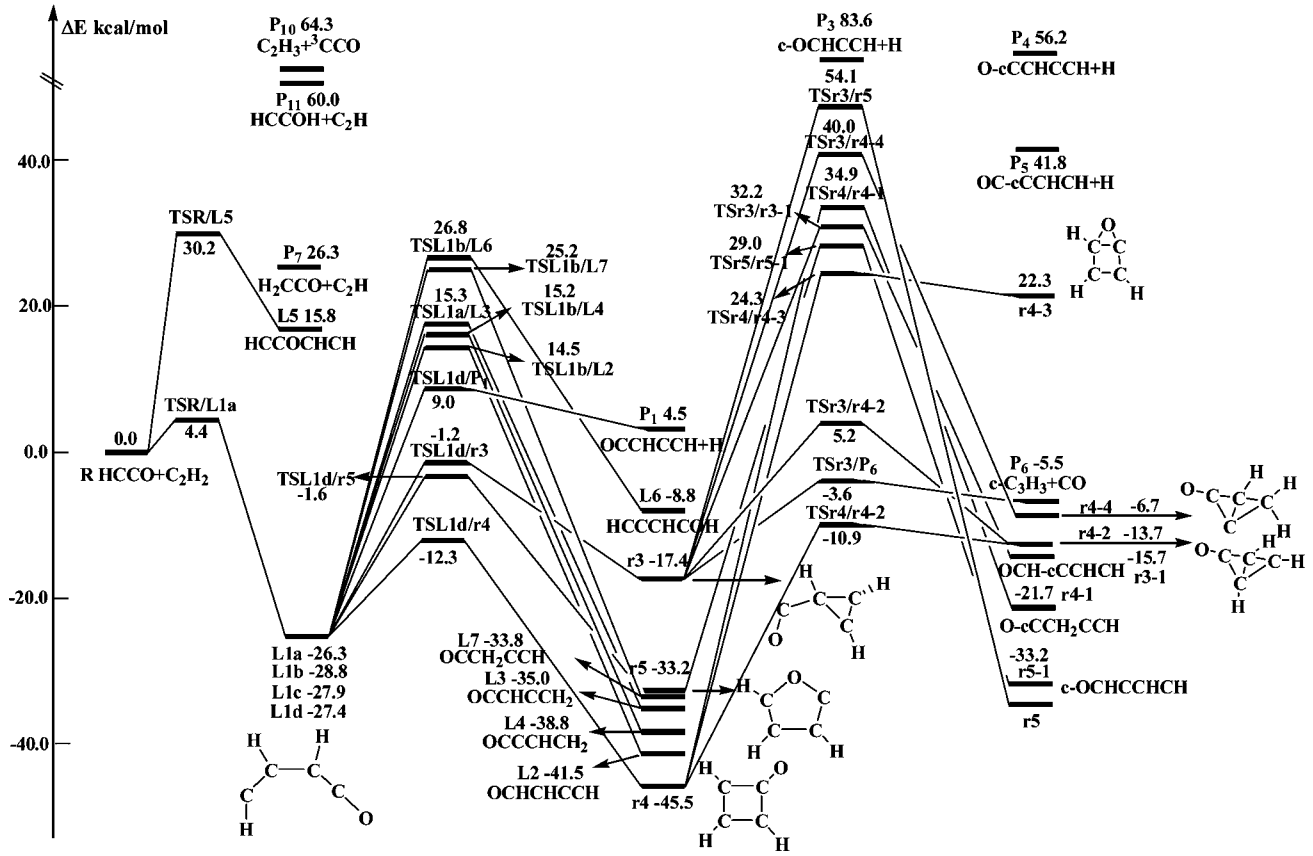

Figure 2. Schematic potential energy surface of the HCCO + C_2H_2 reaction at the G3B3//B3LYP/6-31G(d) level.

isomer **r4**, only **TSr4/r4−2** (−10.9) for conversion to isomer **r4−2**(−13.7) lies lower than the entrance **TSR/L1a** (4.4). Yet, **r4−4** can very easily isomerize back to **r4** instead of rearrangement to others. The other processes for **r4** can surely be excluded due to the rather high-energy products or transition states, that is, H-extrusion to $\mathbf{P_4}$ O−cCCHCCH (56.2), H-migration to O−cCCH$_2$CCH **r4−1** (−21.7) via **TSr4/r4−1** (34.9), and cOCCHCHCH **r4−3** (22.3) via **TSr4−3** (24.3). For isomer **r5**, only one isomerization process to form **r5−1** c-OCHCCHCH (−33.2) via **TSr5/r5−1** (29.0) is located and processes to form $\mathbf{P_3}$ cOCCHCCH + H (83.6) are considered. These two processes can also be excluded due to high transformation energy barriers or high-energy products. So, all in all, for **r4** and **r5**, all transformation pathways have little contribution to the final fragmentation. They will not be considered further.

The intermediate OC−cCHCHCH (−17.4) **r3** has six evolution channels: (i) C−C rupture to form $\mathbf{P_6}$ cCHCHCH + CO (−5.5) via **TSr3/P$_6$** (−3.6); (ii) 1,2-H-shift leading to **r3−1** OCH−cCCHCH (−15.7) via **TSr3/r3−1**; (iii) H-extrusion to form $\mathbf{P_5}$ OC−cCCHCH + H (41.8); (iv) ring-closure leading to **r4−2** (−13.7) via **TSr3/r4−2**; (v) and (vi) isomerization leading to **r4−4** (−6.7) and **r5** (−32.2) via **TSr3/r4−4** (40.0) and **TSr3/r5** (54.1), respectively. The values in parentheses are relative energies in kcal/mol with reference to **R**. Surely, channel (i) is the most favorable reaction channel. Transition states or products involved in the other processes are much higher than reactant **R**. They have little contribution to the final fragments.

3.3. Reaction Mechanism and Implications. In summary, the most possible product pathway for the HCCO + C_2H_2 reaction at the G3B3//B3LYP/6-31G(d) level can be written as

$$\mathbf{R}\ \mathrm{HCCO} + \mathrm{C_2H_2} \rightarrow \mathrm{HCCHCHCO}\ \mathbf{L1} \rightarrow \mathrm{OC{-}cCHCHCH}\ \mathbf{r3} \rightarrow \mathbf{P_6}\ \mathrm{cCHCHCH} + \mathrm{CO}$$

Formation of **L1** is the rate-determining step via **TSR/L1a** (4.4). The intermediates, transition states, and fragments all lie lower than **R** and **TSR/L1a**. The α-C-addition isomer HCCH-CHCO **L1** resides in a considerable potential well, that is, the lowest barrier toward fragmentation to $\mathbf{P_6}$ is just 5.6 kcal/mol lower than that toward dissociation back to the reactant **R**. Thus, the rate constants for HCCO + C_2H_2 should show distinct pressure-dependent effects. This has not been considered in previous experiments.

The rate-determining α-C-addition barrier is 4.4 and 5.3 kcal/mol at the G3B3//B3LYP/6-311++G(d,p) and G3B3//QCISD/6-31G(d) levels, respectively. Due to the existence of a considerable entrance barrier, the HCCO + C_2H_2 reaction can play a role in the high-temperature C_2H_2/O combustions, particularly when the C_2H_2 is excessive. Also, the HCCO radical is the major product of the NCO reactions with C_2H_2 and other alkynes. Thus, in the high-temperature zones, the HCCO + C_2H_2 reaction should be taken into account in estimating the removal rates of the NCO and C_2H_2 species.

One interesting finding is the formation of the exclusive fragmentation product $\mathbf{P_6}$ *c*-C_3H_3 + CO. Although the cyclic C_3H_3 radical is energetically higher (by 34.7 kcal/mol) than the linear form (*l*-C_3H_3), their interconversion is prohibited by high barriers (33.0 kcal/mol) at the CASPT2//B3LYP/6-31G(d,p) level.[41] Note that $\mathbf{P_6}$ lies only 5.5 kcal/mol below the reactant **R** HCCO + C_2H_2. Even the released heat (20.7 kcal/mol at the G3B3//B3LYP/6-31G(d) level) from the ^{3}O + C_2H_2 → HCCO + H reaction is completely transformed into the HCCO radical, it is still not enough to drive the *c*-C_3H_3 → *l*-C_3H_3 conversion. In one early experimental study on the oxidation of C_2H_2 by O-atoms, detection of the $C_3H_3^+$ ion suggests the formation of the C_3H_3 radical.[25] It was proposed to be formed either via the $^3CH_2$ + C_2H_2 or HCCO + C_2H_2 reaction. Yet, we argue that

TABLE 1: Total (au) and Relative Energies in Parentheses (kcal/mol) of the Reactant, Intermediate Isomers, Products, and Transition States at the G3B3//B3LYP/6-31G(d) and G3B3//B3LYP/6-311++G(d,p) Levels

species	G3B3//B3LYP/ 6-31G(d)	G3B3//B3LYP/ 6-311++G(d,p)
R HCCO + C_2H_2	−229.1216788(0.0)	−229.1210465(0.0)
L1a OCCHCHCH	−229.1636175(−26.3)	−229.1642147(−27.1)
L1b OCCHCHCH	−229.1675124(−28.8)	−229.1680266(−29.5)
L1c OCCHCHCH	−229.1661483(−27.9)	−229.1667255(−28.7)
L1d OCCHCHCH	−229.1653869(−27.4)	−229.1658887(−28.1)
L2 OCHCHCCH	−229.1878137(−41.5)	−229.1880455(−42.0)
L3 OCCHCCH_2	−229.1774855(−35.0)	−229.1781178(−35.8)
L4 OCCCHCH_2	−229.1835532(−38.8)	−229.1787812(−36.2)
L5 HCCOCHCH	−229.0964529(15.8)	−229.0964744(15.4)
L6 HCCCHCOH	−229.1357696(−8.8)	−229.135608(−9.1)
L7 HCCCH_2CO	−229.1755976(−33.8)	−229.1758008(−34.4)
r3 OC−cCHCHCH	−229.1493911(−17.4)	−229.149925(−18.1)
r4 O−cCCHCHCH	−229.1941769(−45.5)	−229.1945605(−46.1)
r5 cOCCHCHCH	−229.1745598(−33.2)	−229.1751409(−33.9)
r3−1 OCH−CCHCH	−229.1466722(−15.7)	−229.1471774(−16.4)
r4−1 O−cCCH_2CCH	−229.1563318(−21.7)	−229.1569862(−22.6)
r4−2 O−cCCH−CHCH	−229.1436304(−13.7)	−229.1443992(−14.7)
r4−3 cOCCH−CHCH	−229.0861061(22.3)	−229.0866283(21.6)
r4−4 O−cCC−CHCH_2	−229.1324096(−6.7)	−229.1331316(−7.6)
r5−1 c-OCHCCHCH	−229.1745358(−33.2)	−229.1750977(−33.9)
TSR/L5	−229.0734728(30.2)	−229.0740704(29.5)
TSR/L1a	−229.1146974(4.4)	−229.1139843(4.4)
TSL1a/L3	−229.097329(15.3)	−229.0978685(14.5)
TSL1d/P_1	−229.1073526(9.0)	−229.1072786(8.7)
TSL1d/r4	−229.1413277(−12.3)	−229.1416703(−12.9)
TSL1d/r3	−229.1236028 (−1.2)	−229.1240347(−1.9)
TSL1d/r5	−229.1241935(−1.6)	−229.1243296(−2.1)
TSL1b/L4	−229.0973944(15.2)	−229.0991986(13.7)
TSL1b/L2	−229.0985241(14.5)	−229.0981658(14.4)
TSL1b/L6	−229.0789284(26.8)	−229.07913482(26.3)
TSL1/L7	−229.0815936(25.2)	−229.0819695(24.5)
TSL1b/L1c	−229.1612399(−24.8)	−229.1616569(−25.5)
TSL1a/L1d	−229.1592695(−23.6)	−229.1596451(−24.2)
TSL1a/L1c	−229.160717(−24.5)	−229.1612199(−25.2)
TSL1b/L1d	−229.1603838(−24.3)	−229.1608385(−25.0)
TSr3/r3−1	−229.0704099(32.2)	−229.0707681(31.6)
TSr3/P_6	−229.1274407(−3.6)	−229.1265722(−3.5)
TSr3/r4−2	−229.1133129(5.2)	−229.1136183(4.7)
TSr3/r5	−229.0355234(54.1)	−229.0583872(39.1)
TSr3/r4−4	−229.0579722(40.0)	−229.0362372(53.2)
TSr4/r4−1	−229.066072(34.9)	−229.0666266(34.1)
TSr4/r4−2	−229.1391158(−10.9)	−229.1398044(−11.8)
TSr4/r4−3	−229.0830228(24.3)	−229.0835878(23.5)
TSr5/r5−1	−229.0755082(29.0)	−229.0752048(28.8)
P_1 OCCHCCH + H	−229.1144685(4.5)	−229.1144447(4.1)
P_2 CCHCHCH + ^{3}O	−228.9299456(120.3)	−228.9303171(119.7)
P_3 c-OCCHCCH + H	−228.9884565(83.6)	−228.9896386(82.5)
P_4 O−cCCHCCH + H	−229.0321766(56.2)	−229.0326372(55.5)
P_5 OC−cCCHCH + H	−229.0550615(41.8)	−229.0553509(41.2)
P_6 cCHCHCH + CO	−229.1304634(−5.5)	−229.1304801(−5.9)
P_7 H_2CCO + C_2H	−229.0797465(26.3)	−229.0773436(27.4)
P_8 C_3H_2 + HCO	−229.0523572(43.5)	−229.0542071(41.9)
P_{10} C_2H_3 + ^{3}CCO	−229.0192548(64.3)	−229.0196929(63.6)
P_{11} HCCOH + C_2H	−229.0260709(60.0)	−229.0230227(61.5)

the HCCO + C_2H_2 reaction should have a major contribution to the observed $C_3H_3^+$ ion on the basis of the following facts: (1) the $^3CH_2$ + C_2H_2 reaction leading to *l*-C_3H_3 is much slower than the HCCO + C_2H_2 reaction leading to *c*-C_3H_3 because the former reaction has a higher entrance barrier (6.7 kcal/mol at the G2M(CC)[32] and 5.5 kcal/ mol at the G3B3//B3LYP/6-31G(d) levels, respectively) than the latter (4.4 kcal/mol at the G3//B3LYP/6-31G(d) level); (2) in the ^{3}O + C_2H_2 reaction, HCCO has been predicted to have a larger abundance than ^{3}-CH_2.[28] Thus, during the combustion of the C_2H_2/O complex systems, the HCCO + C_2H_2 reaction should play a more important role than the $^3CH_2$ + C_2H_2 reaction.

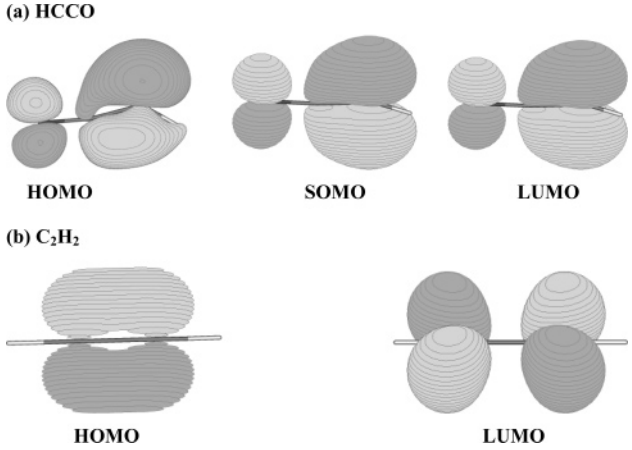

Figure 3. HOMO, SOMO, and LUMO orbital diagrams of reactants.

The present computational study leads us to propose that the HCCO + C_2H_2 reaction can provide an efficient route to form the cyclopropenyl radical (*c*-C_3H_3). We are aware that although the substituted *c*-C_3XYZ radicals (e.g., X = C_4H_9, Y ≃ C_5H_{11}, and Z = H) have been characterized,[42] the parent *c*-C_3H_3 is still unknown in the laboratory. Yet, as the simplest cyclic conjugated radical, *c*-C_3H_3 has been the longstanding subject of numerous theoretical investigations on its structures and energetics.[43] By contrast, the *l*-C_3H_3 has been well characterized experimentally[44] and its reactions have also been studied.[45] The unavailability in the laboratory has blocked the further study on the interesting radical *c*-C_3H_3. The present work may open a new way for future study of the *c*-C_3H_3 chemistry.

Due to the existence of the entrance barrier (around 4 kcal/mol), the title reaction in the gas phase may not occur in space where the temperature is usually very low (less than 100 K). Yet on the iced surface or in the ice grain, the title reaction may be effectively catalyzed to occur.

3.4. Reliability Assessment. The above discussions are based on the G3B3//B3LYP/6-31G(d) calculations. This method has been proved to provide very accurate thermochemical energetics.[35,36] The most possible error may come from the geometries based on the low-level B3LYP/6-31G(d). Thus, we performed additional calculations using the B3LYP method with larger basis set [6-311++G(d,p)] and the more cost-expensive correlated QCISD method with the same basis set [6-31G(d)]. As shown in Table 1, the G3B3//B3LYP/6-311++G(d,p) relative energies for a total of 54 species are very close to the corresponding G3B3//B3LYP/6-31G(d) values. The largest deviation is 1.6 kcal/mol for **L4**, which is in the range of quantum chemical computational error. Moreover, the G3B3//QCISD/6-31G(d) relative energies for **L1a, TSR/L1a, TSL1d/r3, TSL1d/r4, TSL1d/r5, r3, and TSr3/P_6** are calculated to be −26.2, 5.3, −1.0, −12.3, −1.4, −17.3, and −2.7 kcal/mol, respectively. They are also close to the corresponding G3B3//B3LYP/6-31G(d) values. Therefore, it is suitable to chose the G3B3//B3LYP/6-31G(d) method for the study of the mechanism of the present HCCO + C_2H_2 reaction.

4. Conclusion

A detailed quantum chemical study is performed on the mechanism of the HCCO + C_2H_2 reaction, which has never been studied by theoretics. The general potential energy surface information is obtained at the G3B3//B3LYP/6-31G(d) level. The critical species are recalculated at higher levels including G3B3//B3LYP/6-311++G(d,p) and G3B3//QCISD/6-31G(d). The results indicate that the exclusive fragmentation pathway

is the direct α-C-addition forming the intermediate OCCH-CHCH followed by a 1,3-ring-closure leading to OC−cCH-CHCH before the final dissociation to product $\mathbf{P_6}$ *c*-C_3H_3 + CO. It is demonstrated that *c*-C_3H_3 should be responsible for the observed $C_3H_3^+$ ion in one early experiment, and the title reaction should have a greater contribution than the $^3CH_2$ + C_2H_2 reaction during the C_2H_2/O combustion systems. Moreover, the predominance of $\mathbf{P_6}$ from the HCCO + C_2H_2 reaction suggests that this reaction could be a useful precursor for generating the long-sought cyclopropenyl radical (*c*-C_3H_3), which is the simplest cyclic conjugate radical and has been the longstanding subject of a large number of theoretical investigations. Future experiments are greatly desired for this interesting reaction.

Acknowledgment. This work is supported by the National Natural Science Foundation of China (No. 20103003, 20573046), Excellent Young Teacher Foundation of Ministry of Education of China, and Excellent Young People Foundation of Jilin Province.

Note Added after ASAP Publication. This Article was published on Articles ASAP on May 11, 2006. "Cyclopropyl" in the title and elsewhere was changed to "Cyclopropenyl". The corrected Article was reposted on May 11, 2006.

References and Notes

(1) Grebe, J.; Homann, K. H. *Ber. Bunsen-Ges. Phys. Chem.* **1982**, *86*, 581.
(2) Grebe, J.; Homann, K. H. *Ber. Bunsen-Ges. Phys. Chem.* **1982**, *86*, 587.
(3) Devriendt, K.; Peeters, J. *J. Phys. Chem. A* **1997**, *101*, 2546.
(4) Peeters, J.; Devriendt, K. *Symp. (Int.) Combust. [Proc.]* **1996**, *26*, 1001.
(5) Marinov, N. M.; Pitz, W. J.; Westbrook, C. K.; Castaldi, M. J.; Senkan, S. M. *Combust. Sci. Technol*. **1996**, *21*, 116.
(6) McEnally, C. S.; Pfefferle, L. D. *Combust. Flame* **2000**, *121*, 575.
(7) Peeters, J.; Boullart, W.; Devriendt, K. *J. Phys. Chem.* **1995**, *99*, 3583.
(8) Phippen, D. E.; Bayes, K. D. *Chem. Phys. Lett.* **1989**, *164*, 625.
(9) Blauwens, J.; Smets, B.; Peeters, J. *Symp. (Int.) Combust. [Proc.]* **1976**, *16*, 1055.
(10) Boullart, W.; Nguyen, M. T.; Peeters, J. *J. Phys. Chem.* **1994**, *98*, 8036.
(11) Kilpinen, P.; Glarborg, P.; Hupa, M. *Ind. Eng. Chem. Res.* **1992**, *31*, 1477.
(12) Dagaut, P.; Luche, J.; Cathonnet, M. *Int. J. Chem. Kinet*. **2000**, *32*, 365.
(13) Dagaut, P.; Lecomte, F.; Chevailler, S.; Cathonnet, M. *Combust. Flame* **1999**, *19*, 494.
(14) Peeters, J. *Bull. Soc. Chim. Belg*. **1997**, *106*, 337.
(15) Turner, B. E., Sears, T. J., *Astrophys. J., Part 1* (ISSN 0004-637X), **1989**, *340*, 900.
(16) Kaiser, R. T. *Chem. Rev.* **2002**, *102*, 1309.
(17) Osborn, D. L.; Mordaunt, D. H.; Choi, H.; Bise, R. T.; Neumark, D. M.; Rohlfing, C. M. *J. Chem. Phys*. **1997**, *106*, 10087.
(18) Unfried, K. G.; Glass, G. P.; Curl, R. F. *Chem. Phys. Lett*. **1991**, *177*, 33.
(19) Mordaunt, D. H.; Osborn, D. L.; Choi, H.; Bise, R. T.; Neumark, D. M. *J. Chem. Phys*. **1996**, *105*, 6078.
(20) Endo, Y.; Hirota, E. *J. Chem. Phys*. **1987**, *88*, 4319.
(21) Brock, L. R.; Mischler, B.; Rohlfing, E. A. *J. Chem. Phys*. **1997**, *07*, 665.
(22) Brock, L. R.; Mischler, B.; Rohlfing, E. A. *J. Chem. Phys*. **1999**, *110*, 6773.
(23) Unfried, K. G.; Curl, R. F. *J. Mol. Spectrosc*. **1991**, *150*, 86.
(24) Meyer, J. P.; Hershbrger, J. F. *J. Phys. Chem. A* **2005**, *109*, 4772 and references therein.
(25) Murray, K. K.; Unfried, K. G.; Glass, G. P.; Curl, R. F. *Chem. Phys. Lett*. **1992**, *192*, 512 and references therein.
(26) Wei, Z. G.; Huang, X. R.; Sun, Y. B.; Sun, C. C. *Chem. J. Chin. Univ.* **2004**, *25*, 1504.
(27) Tokmakov, I. V.; Moskaleva, L. V.; Paschenko, D. V.; Lin, M. M. *J. Phys. Chem. A* **2003**, *107*, 1066 and references therein.
(28) Chikan, V.; Lenoe, S. R. *J. Phys. Chem. A* **2005**, *109*, 2525 and references therein.
(29) Boullart, W.; Peeters, J. *J. Phys. Chem.* **1992**, *96*, 9810 and references therein.
(30) Becher, K. H.; Kurtenbach, R.; Schmidt, F.; Wiesen, P. *Chem. Phys. Lett*. **1995**, *235*, 230−234.
(31) Xie, H. B.; Ding, Y. H.; Sun, C. C. Unpublished results.
(32) Le, T. N.; Lee, H. Y.; Mebel, A. M.; Kaiser, R. I. *J. Phys. Chem. A* **2001**, *105*, 1847.
(33) Frisch, M. J.; Trucks, G. W.; Schlegel, H. B.; et al. *GAUSSIAN 98*, Revision A.11; Gaussian, Inc.: Pittsburgh, PA, 1998.
(34) Curtiss, L. A.; Raghavachari, K.; Redfern, P. C.; Rassolov, V.; Pople, J. A. *J. Chem. Phys*. **1998**, *109*, 7764.
(35) Boboul, A. G.; Curtiss, L. A.; Redfern, P. C.; Raghavachari, K. *J. Chem. Phys*. **1999**, *110*, 7650.
(36) (a) Performance of the B3LYP functional for geometry optimization was assessed, for example, by the authors of several versatile model chemistries: G2(B3LYP/MP2/CC) (Bauschlicher, C. W.; Partridge, H. *J. Chem. Phys*. **1995**, *103*, 1788), G2M (Mebel, A. M.; Morokuma, K.; Lin, M. C. *J. Chem. Phys*. **1995**, *103*, 7414), G3//B3LYP (Baboul, A. G.; Curtiss, L. A.; Redfern, P. C.; Raghavachari, K. *J. Chem. Phys*. **1999**, *110*, 7650), and G3X (Curtiss, L. A.; Redfern, P. C.; Raghavachari, K.; Pople, J. A. *J. Chem. Phys*. **2001**, *114*, 108). (b) Xie, H. B.; Ding, Y. H.; Sun, C. C. *J. Phys. Chem. A* **2005**, *109*, 8419. (c) Xie, H. B.; Ding, Y. H.; Sun, C. C. *J. Theor. Comput. Chem*. **2005**, *4*, 1029. (d) Tokmakov, I. V.; Lin, M. C. *J. Phys. Chem. A* **2002**, *106*, 11309.
(37) Wittbrodt, J. M.; Schlegel, H. B. *J. Chem. Phys.* **1996**, *105*, 6574−6577.
(38) Lau, K. C.; Liu, Y.; Butler, L. J. *J. Chem. Phys*. **2005**, *123*, 054322.
(39) Zou, P.; Osborn, D. L. *Phys. Chem. Chem. Phys*. **2004**, *6*, 1697.
(40) (a) Chen, H. T.; Ho, J. J. *J. Phys. Chem*. **2003**, *107*, 7004. (b) Chen, H. T.; Ho, J. J. *J. Phys. Chem. A* **2003**, *107*, 7643.
(41) Vereechen, L.; Pierloot, K.; Peeters, J. *J. Chem. Phys*. **1998**, *108*, 1068.
(42) Cano, M.; Quintana, J.; Juliá, L.; Camps, F.; Joglar, J. *J. Org. Chem*. **1999**, *64*, 5096.
(43) Closs, G. L.; Evanochko, W. T.; Norris. J. R. *J. Am. Chem. Soc*. **1982**, *104*, 350 and references therein.
(44) Yuan, L.; Desain, J. D.; Curl, R. F. *J. Mol. Spectrosc*. **1998**, *187*, 102 and references therein.
(45) Geppert, W. D.; Eskola, A. J.; Timonen, R. S.; Halonen, L. *J. Phys. Chem. A* **2004**, *108*, 4232 and references therein.